Composites Part B 268 (2024) 111080

Contents lists available at ScienceDirect

Composites Part B

journal homepage: www.elsevier.com/locate/composites

# Strain rate and temperature dependence of short/unidirectional carbon fibre PEEK hybrid composites

James Pheysey [a,b], Francesco De Cola [b], Antonio Pellegrino [c,d], Francisca Martinez-Hergueta [a,*]

[a] School of Engineering, Institute of Infrastructure and Environment, The University of Edinburgh, Sanderson Building, Robert Stevenson Road, Edinburgh, EH9 3FB, Scotland, United Kingdom

[b] WAE Technologies Limited, Grove, Wantage, Oxfordshire, OX12 0DQ, England, United Kingdom

[c] Department of Engineering Science, University of Oxford, Parks Road, Oxford, OX1 3PJ, England, United Kingdom

[d] University of Bath, Department of Mechanical Engineering, North Rd, Claverton Down, Bath BA2 7AY, England, United Kingdom

ARTICLE INFO

*Keywords:*
Strain-rate dependency
Temperature dependency
Dynamic response
Thermoplastic carbon fibre composites
Hybrid composites

ABSTRACT

Short fibre and hybrid carbon fibre PEEK composite materials were tested in tension and compression under quasi-static and high strain rate conditions to observe the strain rate dependence. Multiple temperatures including room temperature, +85 and −50 °C were used to investigate the temperature dependence of the materials. The hybrid laminate comprised a consolidated short fibre core reinforced with outer UD plies in the 0° orientation to provide maximum reinforcement whilst minimising the quantity of expensive UD composite used. Under compression, the beneficial effect of the hybridisation strategy was observed for all high-strain rate testing conditions, where the hybrid laminate outperformed the response of the individual constituents in terms of strength and strain rate dependency. The outer unidirectional (UD) layers contributed to confining the short fibre core, providing superior structural integrity. Under tension, the response was dominated by the UD layers with a 288% increase in strength at room temperature over the short fibre material. However, in the high temperature quasi-static case, the strength was dramatically reduced, by 64%, due to the debonding of the UD reinforcement. This study shows the suitability of hybrid composites for impulsive applications and provides material parameters for the future design of composite structures subjected to impact events.

## 1. Introduction

The automotive industry requires the development of novel high-performance low-cost lightweight materials to reduce emissions. Continuous fibre composite materials are limited to high-cost applications, so they are not a feasible option in the civil automotive industry. Furthermore, conventional thermoset composites present recyclability issues due to the cross-linking in the curing process [1,2], so their adoption is limited by the end-of-life vehicle regulation [3]. Thermoplastic composites offer a fully recyclable solution, however, as a result of the recycling process, the affordable recycled commercial products consist of short-fibre reinforced composites, with lower mechanical performance [4,5]. Hybridisation of short fibre composites with uni-directional (UD) layers have been shown to provide an effective performance increase under quasi-static loading conditions, potentially allowing their use in primary structural components [6,7]. The future implementation of these hybrid composites in the automotive industry requires a detailed understanding of their mechanical response at high strain rates within operating temperatures. This is crucial to design components such as body panels, and crash structures that might be subjected to medium strain rates, up to 25 m/s impact velocities [8].

The dependence of the strain rate on the mechanical properties of composite materials is directly related to the nature of the material and the failure mode. Among the thermoplastic resin systems, Polyether ether ketone (PEEK) is a semi-crystalline thermoplastic with high specific mechanical performance and good impact resistance that might be a suitable candidate for replacing conventional metal components [9,10]. The compressive rate dependence of pure PEEK has been investigated in multiple studies up to 3000 $s^{-1}$ [11–13]. All studies have shown an increased compressive strength as a result of an increase in strain rate. All studies show a minimal change in compressive stiffness with strain rate. These studies have also investigated the temperature dependence of PEEK under compression [11–13]. A decrease in temperature was shown to produce an increased compressive strength due to an increased fractured toughness leading to higher energy brittle fracture [12]. The compressive rate dependence of PEEK short fibre composite has also been investigated, but the scope of those studies is

* Corresponding author.
*E-mail addresses:* ap3551@bath.ac.uk (A. Pellegrino), francisca.mhergueta@ed.ac.uk (F. Martinez-Hergueta).

https://doi.org/10.1016/j.compositesb.2023.111080
Received 4 August 2023; Received in revised form 6 October 2023; Accepted 24 October 2023
Available online 27 October 2023

limited to room temperatures. It has been observed a minimal change in compressive modulus with strain rate, however, compressive yield strength increased 11% when increasing the strain rate from 800 to 1500 $s^{-1}$ [14].

In tension, studies have shown PEEK has a significant strain rate dependence, resulting in increased tensile strength for high strain rates [15,16]. These studies also reviewed the temperature dependence of PEEK, indicating a larger strain rate dependence at higher temperatures, with stiffness and strength being affected. Short carbon fibre PEEK composites have been shown to exhibit a similar rate dependence to pure PEEK with an increased stiffness and strength with increased strain rate [17–19]. At elevated temperatures, an increased strain to failure has been also reported [19].

On the other hand, UD composites shown no rate dependence in longitudinal tension, regardless of the resin system employed (e.g., PEEK or epoxy) [20–22]. A significant tensile temperature dependence has only been observed for UD composites above the glass transition temperature, however, the temperature dependence below that threshold is minimal due to the properties being fibre dominated [23]. In compression, the strain rate dependency of the UD laminates are dominated by the resin rather than fibre dependent. UD epoxy composites have shown a significant strain rate dependence in compression with increases in both compressive stiffness and strength observed [24,25], however, continuous fibre PEEK composites showed a much lower rate dependence [26].

Although significant work was carried out to investigate the strain rate and temperature dependence of PEEK resin, there have been limited studies into the strain rate and temperature dependence of short fibre PEEK composites. In particular, strain rate dependency at low temperatures for compressive and tensile response is a current open research question. Furthermore, to the authors' knowledge, no work has been carried out to study the effect of strain rate and temperature on hybrid composites combining short fibre composite with UD plies. This work looks at strain rate and temperature dependence on the tensile and compressive performance of short carbon fibre PEEK composite, and a hybrid composite produced from UD pre-preg and short carbon fibre PEEK composite. This work aims to understand if the hybrid material has the same strain rate and temperature dependence that would be expected from its constituent elements.

## 2. Experiments

### 2.1. Materials and manufacture

The materials selected for this investigation were carbon fibre-reinforced PEEK thermoplastic composites supplied by Solvay [27]. The first material was a short fibre composite in pellet format with the brand name Ketaspire KT-880 CF30 with an approximate 30% volume fraction of fibres with average fibre diameter and length of 8 μm and 150 μm respectively [7]. The second material was a UD pre-preg denominated APC-2 IM7 with an approximate 68% volume fraction of carbon fibres.

The raw materials were processed into panels through compression moulding using a PEI Lab 450 press with a pressure of 2 MPa [7]. The hybrid material consisted of a core of short fibre composite embedded within two outer layers of UD combined in a second compression moulding step, and final stacking sequence [0/short/0], see Fig. 1. Pure short fibre composite panels and hybrid composite panels were produced as 2 mm thickness plates with a void content of $2.46 \pm 0.33$ measured through acid digestion following BS ISO 14127:2008 Procedure A3. The representative volume element of the short fibre composite has an estimated size of 0.6 mm, 4 times the average fibre length, according to the criteria suggested in [28,29] for short fibre composites with similar fibre volume fractions.

Specimens were extracted using a CNC milling machine with a 5 mm tool. The compressive test samples were machined to a 4 × 4 mm size with a thickness of 2 mm, see Fig. 2(a). Dog bone specimens were machined for tensile experiments with a gauge length of 10 mm, see Fig. 2(b). These reduced dimensions have been previously employed to ensure force equilibrium conditions were achieved under high strain rates, whilst capturing the representative volume element [30,31]. The same sample geometries were used for quasi-static and dynamic testing to ensure that any differences observed were solely due to the strain rate, and not changes in stress concentration within the sample.

**Table 1**
Test matrix for quasi-static and high strain rate testing.

| Test type | Temperature (°C) | Strain rate ($s^{-1}$) | | |
|---|---|---|---|---|
| | | Quasi-static | High rate 1 | High rate 2 |
| Tensile | 23 | 0.01 | 460 | N/A |
| | 85 | 0.01 | 460 | N/A |
| Compression | −50 | 0.01 | 600 | 1350 |
| | 23 | 0.01 | 600 | 1350 |
| | 85 | 0.01 | 600 | 1350 |

### 2.2. Mechanical testing

The testing matrix includes up to three strain rates and three temperatures, see Table 1. A total of 47 tensile and 80 compressive valid experiments were conducted. The methodology for quasi-static and dynamic testing is described in the following sections.

#### 2.2.1. Quasi-static characterisation

A screw-driven Zwick Z250 universal test machine was used for quasi-static tensile and compressive testing. A constant loading rate of 0.1 and 0.04 mm/min was used for tensile and compressive tests respectively, producing a strain rate of approximately 0.01 $s^{-1}$. An environmental chamber was employed to oven-heat the specimen or cool it down with liquid nitrogen, resulting in temperatures of +85 and −50 °C, set by conventional automotive requirements [32]. A Eurotherm 3508 controller was used with a type K thermocouple to control the temperature. A JAI BM-500GE camera (resolution 2058 × 2456 pixels) at a frame rate of 1 fps was used to record the tests. 2D-Digital Image Correlation (DIC) analysis software VIC-2D 6 was utilised to monitor the deformation with white paint speckling applied to the samples. DIC was only used for room temperature and high temperature testing as the liquid nitrogen cloud reduced image quality for the low temperature tests. Strain data for low temperatures was obtained through calibration of the cross-head displacement, which involved loading the test machine to 2.5 kN without a sample, allowing the fixture stiffness to be accounting for in calculation of strain. This method does not take into account non-linearity in strain beyond that load and can induce error above the calibration force. Hence, considering the limitations, the discussion of our study was focused on composite strengths, which do not require strain data. Post-mortem specimens were inspected using a TM4000Plus Scanning Electron Microscope (SEM) with a 15 kV accelerating voltage and a working distance of approximately 10 mm.

#### 2.2.2. Dynamic characterisation

Dynamic testing was carried out using two different Split Hopkinson Bar apparatuses. The Split Hopkinson Pressure Bar (SHPB) utilised for the compression experiments included a striker, input and output bars produced from Ti–6Al–4V, 2.8 m long and 16 mm in diameter. Both bars were supported by low-friction nylon bearings in order to minimise friction, sagging, and lateral movement, as well as ensuring the alignment of the input and output bars. The compressive samples were mounted between flat bar ends with a small amount of silicon grease used to secure the samples. A cardboard pulse shaper mounted at the interface between the striker and the input bar was used to control the rise time of the stress wave. Two different strain rates were imposed, 600 and 1350 $s^{-1}$. A Eurotherm 3508 controller was used with a type

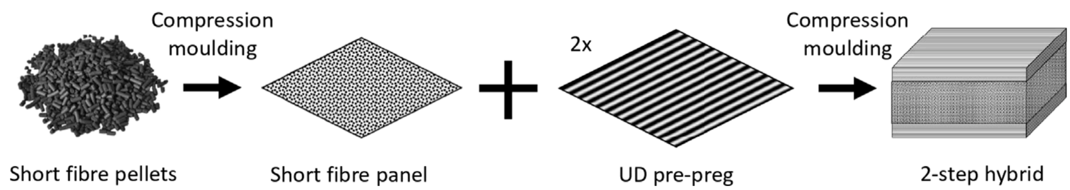


**Fig. 1.** Manufacturing of the hybrid panels by a 2-step compression moulding process.

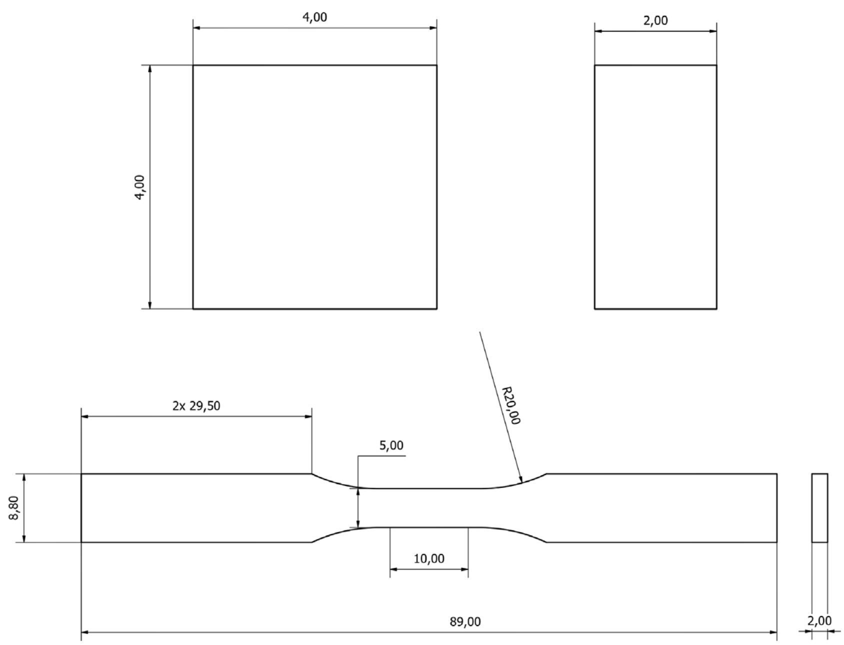


**Fig. 2.** (a) Compression and (b) tensile test specimen dimensions.

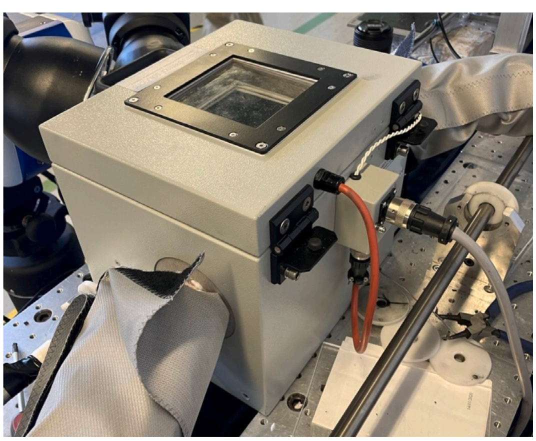

**Fig. 3.** Environmental chamber installed over the SHPB.

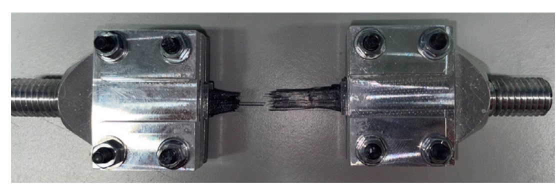

**Fig. 4.** Aluminium clamps used for testing of the hybrid composite in tension.

K thermocouple to monitor the temperature. Sub-ambient temperatures were obtained by connecting a liquid nitrogen dewar to the inlet of the thermal unit while high temperatures were achieved through an oven. The sample enclosure included heated windows to stop condensation forming and record the sample during deformation and failure, see Fig. 3. The input and output bars entered the environmental chamber through metal tubes with glass fibre wadding used to insulate the chamber whilst minimising the friction on the bars.

The dynamic tensile testing was carried out using a Long Tensile Split Hopkinson Bar designed by Gerlach et al. [33]. The input and output bars produced from Ti–6Al–4V were 2.6 m in length and 16 mm in diameter, with the U shaped striker 2.6 m in length with a section diameter of 35 mm. A cardboard pulse shaper was used to trim the stress wave. The short fibre tensile specimens were bonded to metallic end caps with epoxy adhesive according to the procedure in [31]. The hybrid tensile samples were clamped using custom impedance matched clamps manufactured from Al6061 with 8 bolts used to hold the sample between 2 metal surfaces, as shown in Fig. 4. The environmental chamber used during the compressive testing was also used in tension. Strain rates of up to 460 $s^{-1}$ were achieved.

The SHPBs were instrumented with two and one strain gauges in the input and output bars respectively. All strain measurement locations were setup in a modified half bridge configuration. Amplifiers were used to accurately record the signal on the order of millivolts. All the signals were registered through a high frequency oscilloscope and were post processed using a Matlab script using the method of characteristics and D'Alambert's solution of wave equations [34]. A Specialised Imaging Kirana 05M high-speed camera was use to record the deformation and fracture mechanisms. The camera had a resolution of 924 × 768 pixels and a sampling frequency of 300,000 to 500,000 $s^{-1}$ depending on the time duration of the experiment. Samples were speckled and

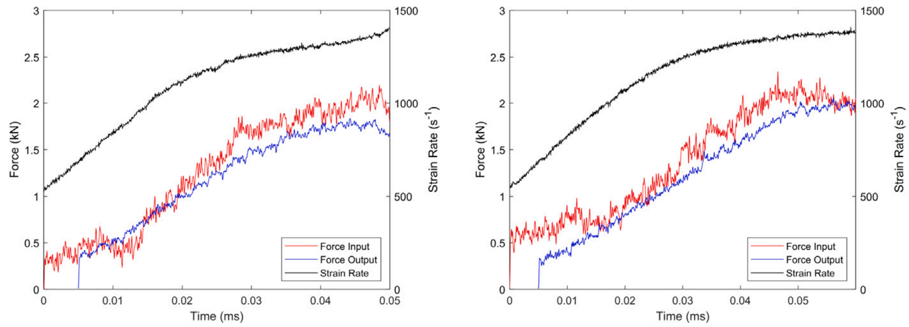


**Fig. 5.** Validation of the force equilibrium for compression at 1350 $s^{-1}$ for the short fibre composite (left) and hybrid composite (right).

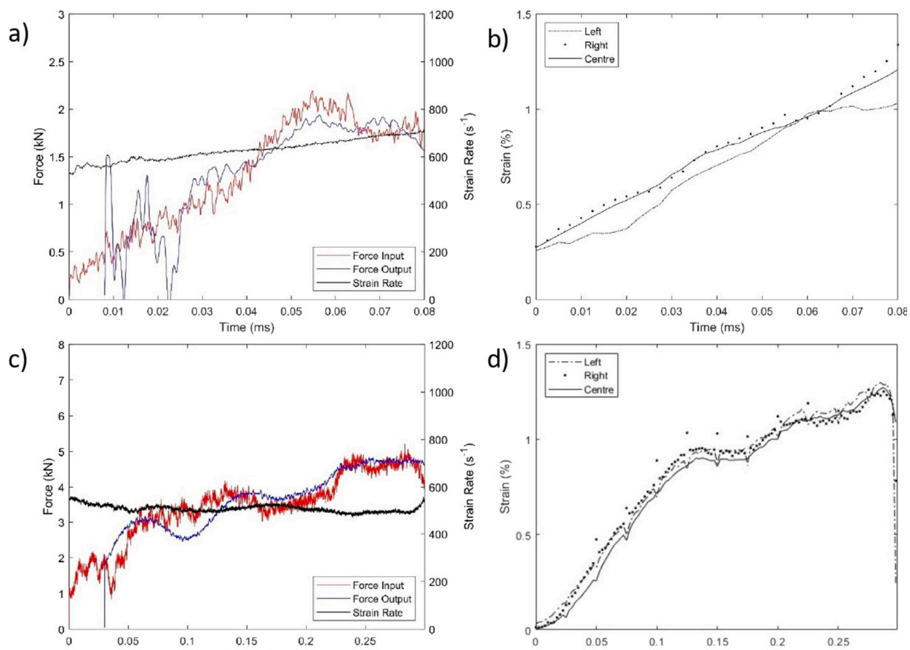


**Fig. 6.** Validation of the force equilibrium for tension. (a) and (c) Input and output bar forces measured through strain gauges. (b) and (d) strain at ends of the gauge length registered by DIC.

2D-DIC analysis software VIC-2D 6 was utilised to monitored the strain field for all high rate tests, since this experimental setup did not present the visibility limitations encountered during quasi-static testing [35].

The dynamic force equilibrium was analysed to validate the dynamic experiments. Fig. 5 plots the forces in the input and output bars against time for the short fibre and hybrid composites tested under compression at 1350 $s^{-1}$. In both cases, the force equilibrium was achieved after approximately 0.015 ms.

In tension, dynamic force equilibrium for strain rates of 460 $s^{-1}$ was achieved at a later stage of the experiment, from 0.03 to 0.04 ms for the short fibre composite, and from 0.1 to 0.2 ms for the hybrid laminate, see Fig. 6(a) and (c). This was a consequence of the larger distance between bar ends to accommodate the specimen and the clamping system. Dynamic force equilibrium was confirmed with the DIC strain measurements. Fig. 6(b) and (d) compare the local strain in the gauge length measured at locations at the input and output ends of the sample.

## 3. Results and discussion

### 3.1. Compressive response

Fig. 7 compares the stress–strain response of the short fibre and hybrid materials for quasi-static and high strain rates. A perceptible strain rate dependency was found for both configurations, resulting in large increments of stiffness and strength, and a reduction in ductility. These results are in agreement with the strain rate dependency of the PEEK resin [36,37], and with the reported strain dependency of short fibre composites [17]. In quasi-static testing, the short fibre composite presented an initial elastic regime followed by a non-linear elastic response until reaching a peak stress at a strain of 5.5%. After this point, a characteristic shear crack propagates, splitting the sample into two bodies. At dynamic strain rates, the development of the shear crack resulted in catastrophic failure.

The behaviour of the hybrid material was very similar to the short fibre material due to the response being matrix dominated, see Fig. 7, however, the UD layers contributed to increasing the stiffness and the strength at the dynamic regime with respect to the short fibre material, likely due to their role in constraining the short fibre core.

Fig. 8 plots the compressive strength as a function of the strain rate of the short fibre composite and the hybrid laminate up to strain rates of 1350 $s^{-1}$. An exponential increase in the strength with the strain rate was registered, according to the expression:

$$\sigma = \sigma_0(1 + \sqrt{K\dot{\varepsilon}}) \tag{1}$$

where $\sigma_0$ is the strength of material under quasi-static testing and $K$ is the fitting parameter to predict the rate dependence [38]. The use of Eq. (1) allows comparison of the strain rate sensitivity of compression and tensile experiments. For the short fibre material the value of $K$

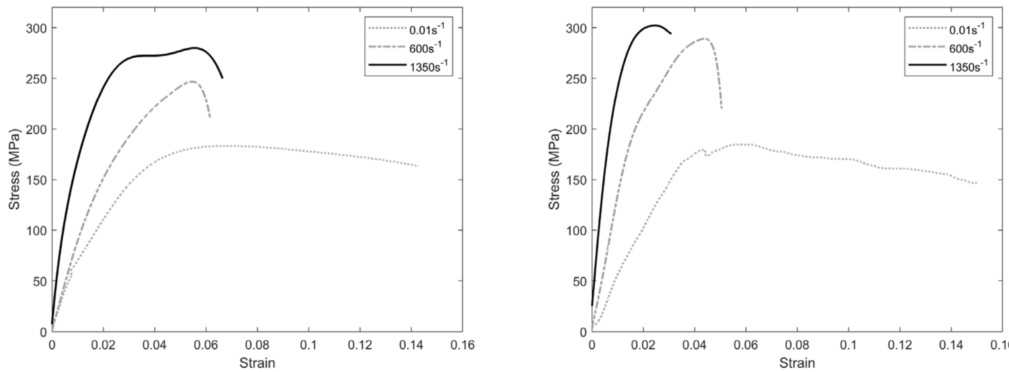


**Fig. 7.** Comparison of compressive stress–strain response under quasi-static and dynamic loading for the short fibre composite (left) and hybrid composite (right).

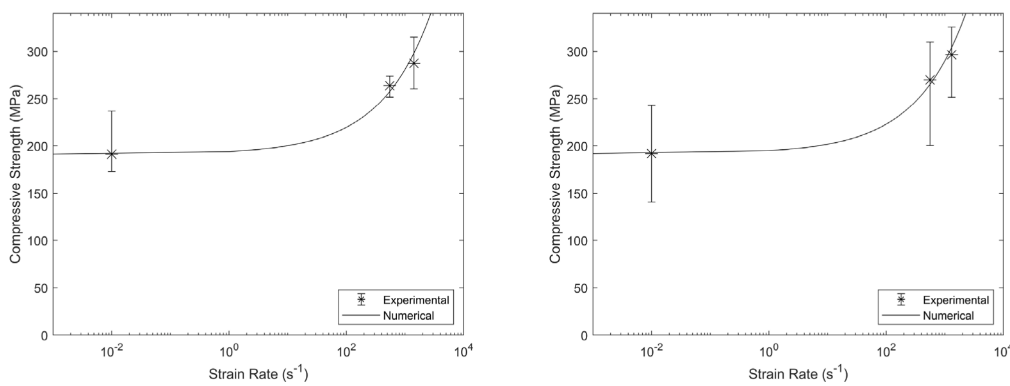


**Fig. 8.** Rate dependence on compressive strength at room temperature for the short fibre composite (left) and hybrid composite (right).

was $2.21 \times 10^{-4}$ s and for the hybrid material K was $2.63 \times 10^{-4}$ s indicating the hybrid was more rate dependent than the short fibre material due to the UD layers constraining the short fibre core under compressive loads. In particular, increases in compressive strength of 45.3% and 55% were observed for the short fibre composite and the hybrid laminate respectively at 1350 s$^{-1}$ compared to the quasi-static values.

The temperature dependence of both composites is shown in Fig. 9. The short fibre composite presented different trends as a function of the strain rate. Under the quasi-static regime, the short fibre material showed a clear temperature dependence with a reduction in strength as temperature increased due to the softening of the PEEK matrix, in agreement with the literature [39,40]. As per SEM observations, a different failure mode was triggered for each temperature, see Fig. 10, main failure mechanisms are highlighted with red arrows. At low temperatures, the material exhibited unstable fibre matrix debonding due to the brittle response of the matrix, in agreement with the previous observations [41,42]. The embrittlement of the resin also led to a higher experimental scattering. The matrix progressively increased the ductility at higher temperatures, suppressing fibre matrix debonding in favour of plastic deformation and final shear failure of the matrix, leading to a stable crack propagation process.

However, at the higher strain rate, the temperature dependence of the short fibre composite was minimal due to a significantly faster fracture resulting in minimal time for matrix cracking to occur before fibre matrix de-bonding. Similarities between the failure modes of composites subjected to low temperatures or high strain rates have been reported in other polymers [43].

Fig. 9 shows the temperature dependence of the hybrid material. Results agree with the short fibre composite where an increased temperature results in a reduced compressive strength due to increased ductility of the resin. It is noted that the variability in strength increased when comparing to the short fibre material. This is due to the difficulty in creating a flat loading surface with such a small sample resulting in different loading paths through the UD and short fibre layers and therefore variability in strength. At the higher strain rate the hybrid material showed the same trend with temperature as in the quasi-static tests due to the UD layers constraining the material and therefore limiting the speed to fracture allowing time for matrix ductility before failure. The hybrid material showed similar strength to the short fibre material in all test conditions confirming the failure as matrix dominated.

Fig. 10(b) shows the failure mechanism of the short fibre composite at room temperature. The composite fails through matrix shearing with plastic deformation clearly observed in the matrix. Fig. 10(c) shows the same failure mechanism as observed at room temperature, matrix shear, for the samples tested at +85 °C, however, an increased level of plastic deformation was observed as PEEK softens with temperature increases including below the glass transition temperature [40]. Fig. 10(a) shows the failure surface tested at −50 °C. The SEM images show brittle failure of the matrix material as previously observed in impact testing at low temperatures [42,44].

SEM images were also used to observe the fracture surfaces of the hybrid composite with a focus on the failure of the UD component of the composite, see Fig. 11. All hybrid materials showed failure in the UD component through fibre breakage. The temperature dependence was not observed in the UD fracture indicating the temperature dependence is a result of the short fibre core, not the UD outer skins.

### 3.2. Tensile stress–strain response

Fig. 12 compares the stress–strain response of the short fibre and hybrid composites for quasi-static and high strain rates. Due to a delay in obtaining dynamic equilibrium, only partial stress–strain curves are plotted for the high strain rate. A significant strain rate dependency was found for the short fibre material, resulting in large increments of stiffness and strength, and a small reduction in ductility. These

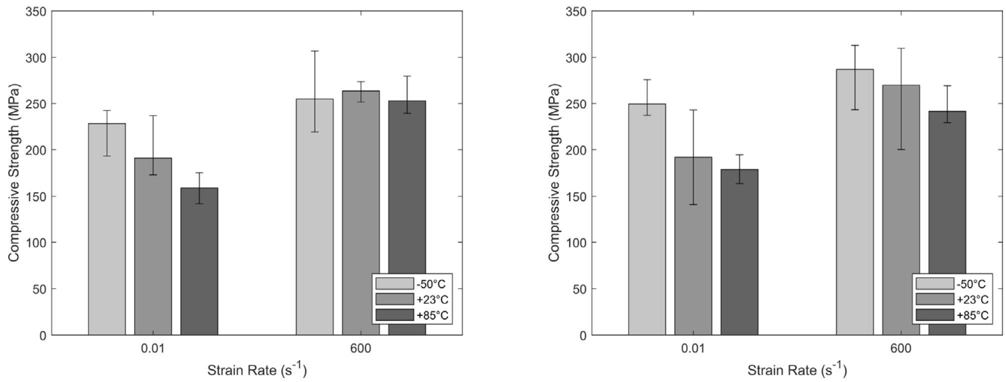


**Fig. 9.** Temperature dependence on compressive strength as a function of the strain rate for the short fibre composite (left) and hybrid composite (right).

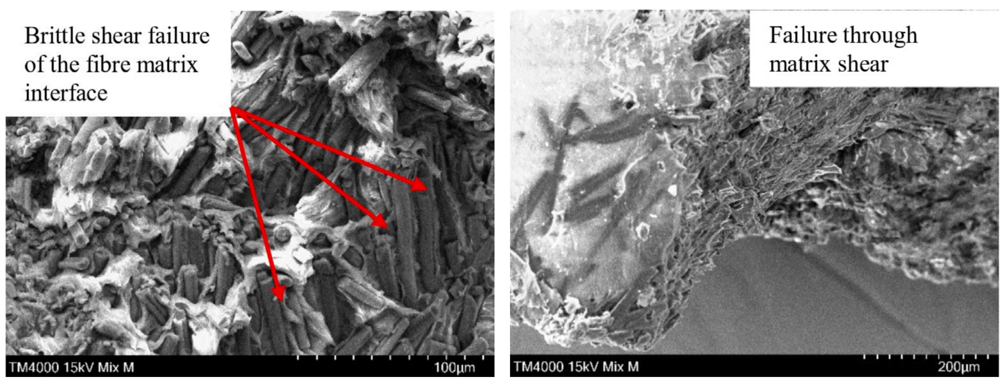


(a) -50°C (b) Room Temperature

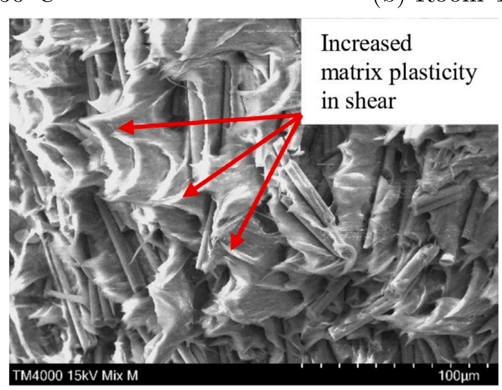


(c) +85°C

**Fig. 10.** SEM images of the fracture surfaces of the short fibre composite subjected to quasi-static compression at different temperatures.

results are in agreement with previous studies in literature [17–19]. The hybrid showed lower rate dependence in agreement with studies looking at rate dependence of UD composites [20]. The short fibre composite presented an initial elastic regime followed by a non-linear elastic response until reaching a peak stress at a strain of 1.6%. After this point, brittle failure occurs resulting in an immediate drop in stress.

The behaviour of the hybrid was significantly different to the short fibre material due to the response being dominated by the UD fibres, see Fig. 12. The hybrid laminate shows a larger linear elastic region with minimal softening before brittle failure of the UD layers occurs.

Fig. 13 plots the tensile strength as a function of the strain rate of the short fibre and the hybrid composites up to strain rates of 460 s$^{-1}$. As previously observed in compression, exponential fitting was performed to predict the rate dependence [38]. Materials both showed high variability at the high strain rate as testing with a split Hopkinson bar produced a range of strain rates and therefore an increased variability in properties. According to Eq. (1), for the short fibre material, the value of K was 8.01 × $10^{-4}$ s, significantly higher than observed in compression. In particular, an increase in tensile strength of 61.3% was observed for the short fibre composite at 460 s$^{-1}$ with respect to the quasi-static values. The hybrid laminate showed no strain rate dependence. This further indicates the failure of the hybrid laminate was dominated by the UD layers, which did not show a strain rate dependency in previous studies [20–22].

The temperature dependence of both composites is shown in Fig. 14. The short fibre composite did not show statistically significant differences in strength in the range of temperatures tested despite exhibiting different failure modes, as per SEM observations, see Fig. 15. However, a reduction in variability was observed at the higher temperature due to the increased matrix ductility improving the defect tolerance of the

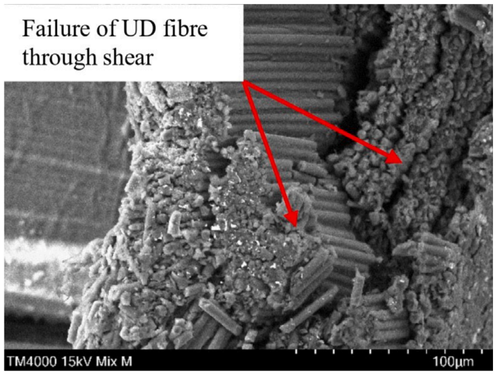


(a) -50°C

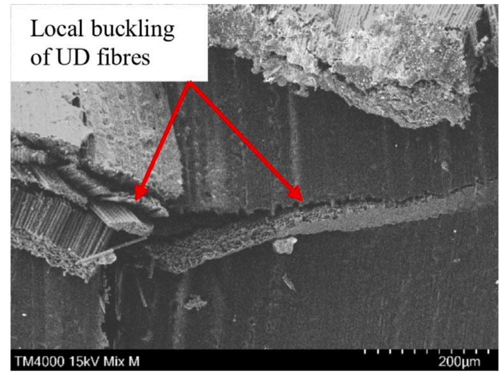


(b) Room Temperature

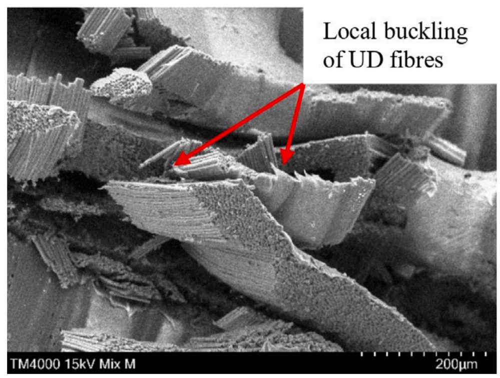


(c) +85°C

**Fig. 11.** SEM images of hybrid composite failure surface through quasi-static compression.

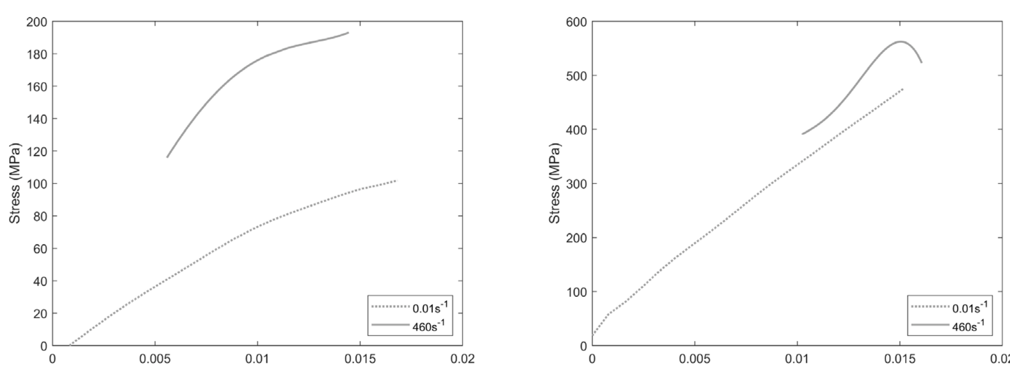


**Fig. 12.** Rate dependence on tensile stress–strain response for the short fibre composite (left) and hybrid composite (right).

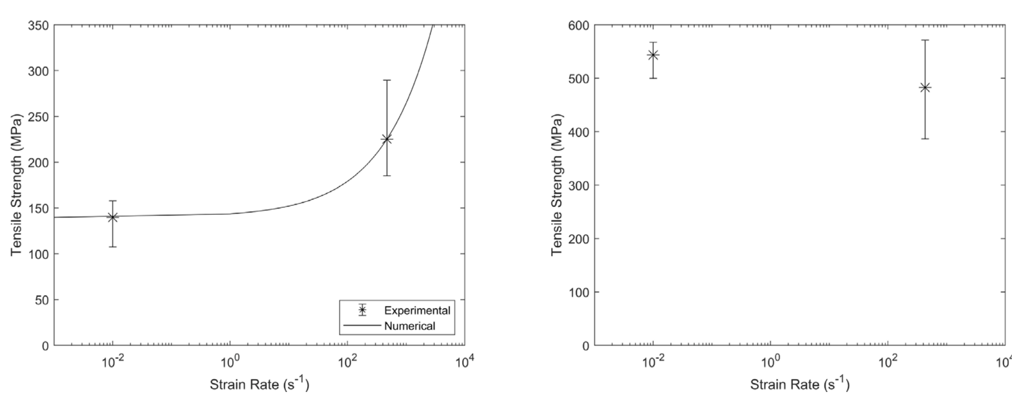


**Fig. 13.** Rate dependence of tensile strength for the short fibre composite (left) and hybrid composite (right).

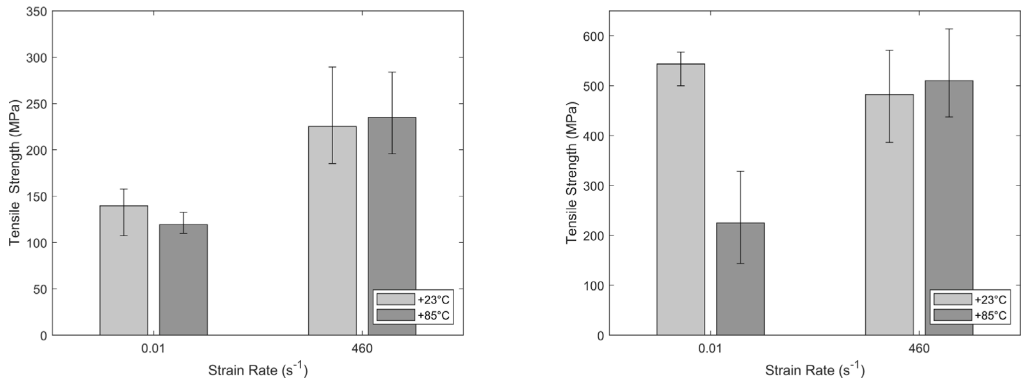


**Fig. 14.** Temperature dependence of tensile strength as a function of the strain rate for the short fibre composite (left) and hybrid composite (right).

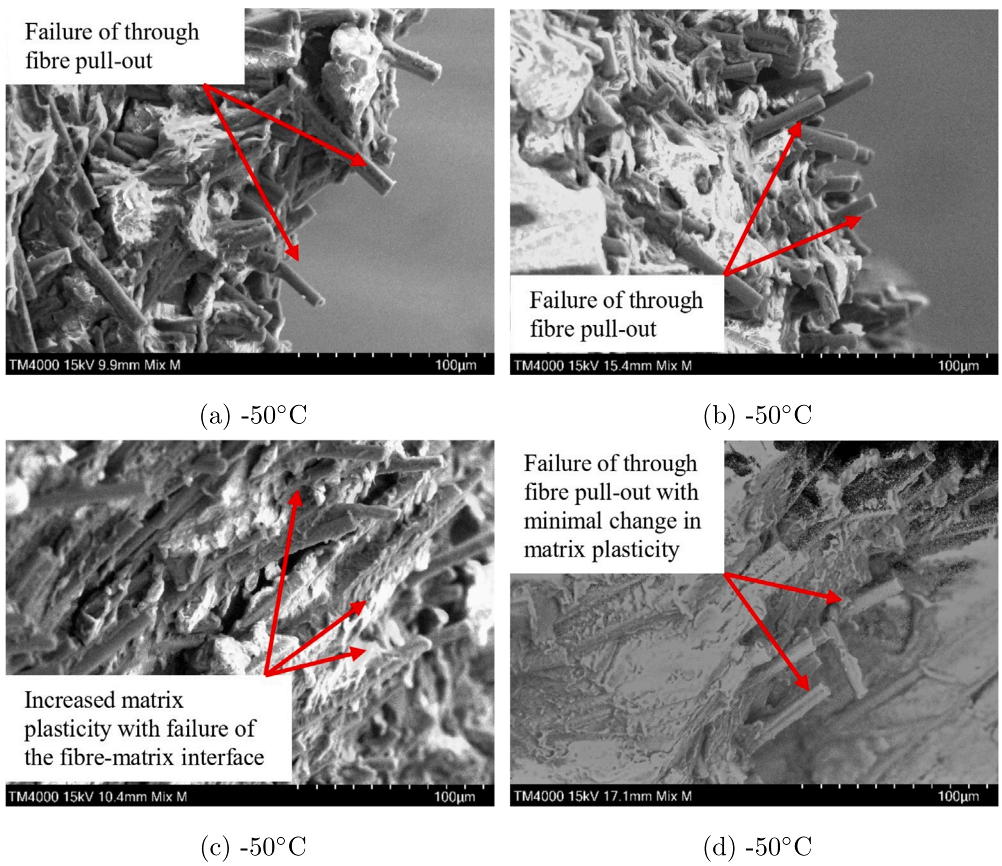


**Fig. 15.** SEM images of short fibre composite failure surface through quasi-static (left) and high rate (right) tension at room temperature (top) and +85 °C (bottom).

material. At quasi-static strain rate, the failure of the composite was driven by fibre-matrix debonding and pull-out, meanwhile, at high strain rate, matrix cracking was the predominant failure mode. No apparent influence of plastic deformation at elevated temperatures was observed, probably due to the predominance of the brittle failure modes at the quasi-static regime, and the faster fracture phenomena at the dynamic regime.

Fig. 14 shows the temperature dependence of the hybrid laminate. Results differ for the short fibre material with a much greater change in strength with increased temperature. Results during quasi-static testing showed a large drop in tensile strength at a higher temperature when compared to those tested at room temperature. This was due to the increased plasticity of the matrix allowing de-bonding between the short fibre and UD layers, severely reducing the load carrying capability of the UD layers, and exhibiting similar strength to the short fibre composite baseline. At the higher strain rate, a negligible temperature dependence was observed due to the higher rate not allowing time for de-bonding of the UD and short fibre layers. A similar effect was observed by Kok et al. where tape debonding occurred in quasi-static testing but did not occur at high strain rate due to reduced failure time [45].

Fig. 15 shows SEM images were taken of all test configurations for the short fibre material. The top left of Fig. 15 shows the fracture surface of a sample tested at room temperature under quasi-static conditions. The main failure mechanism was fibre pull-out with minimal plastic deformation observed in the resin material. The bottom left of Fig. 15 shows the quasi-static fracture surface tested at +85 °C. The matrix surrounding the fibres shows increased plastic deformation indicating an increase matrix ductility as a result of temperature. The high strain rate fracture surface shown on the right of Fig. 15 shows a reduced plastic deformation in the matrix indicating a more brittle failure. Comparing the high strain rate room temperature to the high strain rate at +85 °C, the increased plastic deformation was not observed at the higher temperature due to reduced time for matrix cracking to occur. Similar observations were obtained for the hybrid laminate, with the UD layers failing through fibre breakage in all test conditions and as a result showing no rate dependent changes in fracture surface.

## 4. Conclusions

Strain rate and temperature dependence were investigated for short fibre and hybrid composites manufactured through compression moulding. In compression, both materials showed a clear strain rate dependence with an increased strain rate leading to an increased compressive strength due to reduced fracture time allowing for less matrix cracking before failure through matrix shearing. The short fibre material showed a significant temperature dependence in compression, with increased matrix ductility with temperature, resulting in reduced compressive strength. A reduction in temperature showed the opposite effect with brittle failure in the matrix resulting in an increase in strength. The hybrid material showed similar behaviour to the short fibre material in compressive testing with no relative performance increase resulting from the UD fibre in the hybrid material.

In tensile testing, the short fibre material showed a similar trend to the compressive tests with increased strength at high strain rates. This was due to the high strain rate resulting in a faster fracture allowing a reduced time for matrix cracking before ultimate failure through fibre pull-out. The hybrid material showed a minimal strain rate dependence at room temperature due to the strain rate insensitive UD fibre dominating the failure. At high temperatures, the hybrid showed similar performance at high rates, however, in quasi-static testing the strength was dramatically reduced due to the long test duration allowing for plasticity between the UD and short fibre layers resulting in reduced load carrying capability of the UD fibres.

The beneficial effect of the hybridisation strategy was observed for all high-strain rate testing conditions, where the hybrid laminate outperformed the response of the individual constituents in terms of strength and strain rate dependency. The UD layers contributed to confining the short fibre composite, providing additional structural integrity under compressive loading. This study shows the suitability of this material for impulsive dynamic applications, and provides material data and parameters for the future design of composite structures subjected to impact events.

## CRediT authorship contribution statement

**James Pheysey:** Investigation, Methodology, Formal analysis, Software, Visualisation, Data curation, Validation, Writing – original draft. **Francesco De Cola:** Supervision, Funding acquisition, Project administration, Conceptualisation, Writing – review & editing. **Antonio Pellegrino:** Writing – review & editing, Funding acquisition, Formal analysis, Project administration, Conceptualisation. **Francisca Martinez-Hergueta:** Supervision, Project administration, Conceptualisation, Formal analysis, Funding acquisition, Writing – original draft.

## Declaration of competing interest

The authors declare the following financial interests/personal relationships which may be considered as potential competing interests: Francisca Martinez Hergueta reports financial support was provided by National Manufacturing Institute Scotland.

## Data availability

Data will be made available on request.

## Acknowledgements

The author gratefully acknowledges the PhD funding supplied by WAE Technologies Limited and the National Manufacturing Institute Scotland funded by the Scottish Research Partnership in Engineering [grant number NMIS-IDP/032]. The authors would like to thank the Workshop at The University of Edinburgh for manufacturing the samples, and Stuart Carter at The University of Oxford for manufacturing the clamps.

## References

[1] Post W, Susa A, Blaauw R, Molenveld K, Knoop RJ. A review on the potential and limitations of recyclable thermosets for structural applications. Polym Rev 2020;60(2):359–88.
[2] Pickering SJ. Recycling technologies for thermoset composite materials—current status. Compos A: Appl Sci Manuf 2006;37(8):1206–15.
[3] Regulations: End-of-life vehicles (elvs). 2015, URL https://www.gov.uk/guidance/elv.
[4] Yao S-S, Jin F-L, Rhee KY, Hui D, Park S-J. Recent advances in carbon-fiber-reinforced thermoplastic composites: A review. Composites B 2018;142:241–50.
[5] Bernatas R, Dagréou S, Despax-Ferreres A, Barasinski A. Recycling of fiber reinforced composites with a focus on thermoplastic composites. Clean Eng Technol 2021;5:100272.
[6] Wulfsberg J, Herrmann A, Ziegmann G, Lonsdorfer G, Stöß N, Fette M. Combination of carbon fibre sheet moulding compound and prepreg compression moulding in aerospace industry. Procedia Eng 2014;81:1601–7.
[7] Pheysey J, Teixeira-Dias F, De Cola F, Martinez-Hergueta F. Development of structural low-cost hybrid composites. In: 18th European mechanics of materials conference. 2022.
[8] Abdullah N, Sani M, Salwani M, Husain N. A review on crashworthiness studies of crash box structure. Thin-Walled Struct 2020;153:106795.
[9] Domininghaus H, Haim J, Hyatt D. Plastics for engineers: materials, properties, applications. Hanser Publ 1993 1993;785.
[10] Atkinson J, Hay J, Jenkins M. Enthalpic relaxation in semi-crystalline PEEK. Polymer 2002;43(3):731–5.
[11] Cady C, Blumenthal W, Gray III G, Idar D. Determining the constitutive response of polymeric materials as a function of temperature and strain rate. In: Journal de physique IV (proceedings). vol. 110, EDP sciences; 2003, p. 27–32.
[12] Rae P, Brown E, Orler E. The mechanical properties of poly (ether-ether-ketone)(PEEK) with emphasis on the large compressive strain response. Polymer 2007;48(2):598–615.
[13] El-Qoubaa Z, Othman R. Strain rate sensitivity of polyetheretherketone's compressive yield stress at low and high temperatures. Mech Mater 2016;95:15–27.
[14] Chen C, Zhang C, Zhao Z, Wang Y, Wong S-C, Li Y. Effect of fiber reinforcement and fabrication process on the dynamic compressive behavior of PEEK composites. Int J Mech Sci 2019;155:170–7.
[15] Abbasnezhad N, Khavandi A, Fitoussi J, Arabi H, Shirinbayan M, Tcharkhtchi A. Influence of loading conditions on the overall mechanical behavior of polyether-ether-ketone (PEEK). Int J Fatigue 2018;109:83–92.
[16] Barba D, Arias A, Garcia-Gonzalez D. Temperature and strain rate dependences on hardening and softening behaviours in semi-crystalline polymers: Application to PEEK. Int J Solids Struct 2020;182:205–17.
[17] Kang H, Li Y, Liang J, Thomson D, Cui H, Li Y. Failure of short carbon-fiber-reinforced PEEK composites under high strain rate biaxial loading. Composites B 2022;247:110356.
[18] Chen C, Zhang C, Liu C, Miao Y, Wong S-C, Li Y. Rate-dependent tensile failure behavior of short fiber reinforced PEEK. Composites B 2018;136:187–96.
[19] Tang Z, Chen C, Li A, Deng Y, Zhang C, Li Y. Temperature-and strain-rate-dependent tensile failure behavior of short-fiber-reinforced PEEK composites. Composites B 2023;250:110455.
[20] Weeks C, Sun C. Modeling non-linear rate-dependent behavior in fiber-reinforced composites. Compos Sci Technol 1998;58(3–4):603–11.
[21] Taniguchi N, Nishiwaki T, Kawada H. Tensile strength of unidirectional CFRP laminate under high strain rate. Adv Compos Mater 2007;16(2):167–80.
[22] Shamchi S, Yi X, Moreira PM. Strain-rate dependence of electrically modified unidirectional carbon/epoxy laminates under in-plane tensile loading. Appl Compos Mater 2023;30(1):1–20.
[23] Cao S, Wang X, Wu Z. Evaluation and prediction of temperature-dependent tensile strength of unidirectional carbon fiber-reinforced polymer composites. J Reinf Plast Compos 2011;30(9):799–807.
[24] Hosur M, Alexander J, Vaidya U, Jeelani S. High strain rate compression response of carbon/epoxy laminate composites. Compos Struct 2001;52(3–4):405–17.
[25] Bing Q, Sun C. Modeling and testing strain rate-dependent compressive strength of carbon/epoxy composites. Compos Sci Technol 2005;65(15–16):2481–91.

[26] Pan Z, Yang C, Huang S, Wang M, Wu Z, Gu B. High strain-rate compression behavior of woven CF/PEEK thermoplastic composites at the glassy state and high-elastic state. Int J Mech Sci 2022;235:107740.
[27] Solvay. Material datasheets. 2021.
[28] Harper L, Qian C, Turner T, Li S, Warrior N. Representative volume elements for discontinuous carbon fibre composites–part 1: Boundary conditions. Compos Sci Technol 2012;72(2):225–34.
[29] Harper L, Qian C, Turner T, Li S, Warrior N. Representative volume elements for discontinuous carbon fibre composites–part 2: Determining the critical size. Compos Sci Technol 2012;72(2):204–10.
[30] Cui H, Thomson D, Pellegrino A, Wiegand J, Petrinic N. Effect of strain rate and fibre rotation on the in-plane shear response of ±45 laminates in tension and compression tests. Compos Sci Technol 2016;135:106–15.
[31] Martinez-Hergueta F, Ares D, Ridruejo A, Wiegand J, Petrinic N. Modelling the in-plane strain rate dependent behaviour of woven composites with special emphasis on the non-linear shear response. Compos Struct 2019;210:840–57.
[32] Johnson RW, Evans JL, Jacobsen P, Thompson JR, Christopher M. The changing automotive environment: high-temperature electronics. IEEE Trans Electron Packag Manuf 2004;27(3):164–76.
[33] Gerlach R, Kettenbeil C, Petrinic N. A new split hopkinson tensile bar design. Int J Impact Eng 2012;50:63–7.
[34] De Cola F, Pellegrino A, Glöß ner C, Penumadu D, Petrinic N. Effect of particle morphology, compaction, and confinement on the high strain rate behavior of sand. Exp Mech 2018;58(2):223–42.
[35] Martínez-Hergueta F, Pellegrino A, Ridruejo Á, Petrinic N, González C, LLorca J. Dynamic tensile testing of needle-punched nonwoven fabrics. Appl Sci 2020;10(15):5081.
[36] Hamdan S, Swallowe G. The strain-rate and temperature dependence of the mechanical properties of polyetherketone and polyetheretherketone. J Mater Sci 1996;31(6):1415–23.
[37] Karger-Kocsis J, Friedrich K. Temperature and strain-rate effects on the fracture toughness of poly (ether ether ketone) and its short glass-fibre reinforced composite. Polymer 1986;27(11):1753–60.
[38] Wiegand J. Constitutive modelling of composite materials under impact loading (Ph.D. thesis), Oxford University, UK; 2009.
[39] Chang B, Gu J, Long Z, Li Z, Ruan S, Shen C. Effects of temperature and fiber orientation on the tensile behavior of short carbon fiber reinforced PEEK composites. Polym Compos 2021;42(2):597–607.
[40] Lai Y, Kuo M, Huang J, Chen M. Thermomechanical properties of nanosilica reinforced PEEK composites. In: Key engineering materials. vol. 351, Trans Tech Publ; 2007, p. 15–20.
[41] Gómez-del Rıo T, Zaera R, Barbero E, Navarro C. Damage in CFRPs due to low velocity impact at low temperature. Composites B 2005;36(1):41–50.
[42] Garcia-Gonzalez D, Rodriguez-Millan M, Rusinek A, Arias A. Low temperature effect on impact energy absorption capability of peek composites. Compos Struct 2015;134:440–9.
[43] Siviour C, Walley S, Proud W, Field J. The high strain rate compressive behaviour of polycarbonate and polyvinylidene difluoride. Polymer 2005;46(26):12546–55.
[44] Valentin D, Paray F, Guetta B. The hygrothermal behaviour of glass fibre reinforced pa66 composites: a study of the effect of water absorption on their mechanical properties. J Mater Sci 1987;22(1):46–56.
[45] Kok R, Peroni M, Martinez-Hergueta F, Pellegrino A. Dynamic response of advanced placed ply composites. Composites B 2023;248:110347.